THE JOURNAL OF PHYSICAL CHEMISTRY C

Article

pubs.acs.org/JPCC

# Aged Natural and Synthetic Maya Blue-Like Pigments: What Difference Does It Make?

Enrique Lima,*[,†] Ariel Guzmán,[‡] Marco Vera,[§] Jose Luis Rivera,[†] and Jacques Fraissard[∥]

[†]Instituto de Investigaciones en Materiales, Universidad Nacional Autónoma de México, Circuito exterior s/n, Cd. Universitaria, Del. Coyoacán, CP 04510, México D. F., Mexico

[‡]ESIQIE−Instituto Politécnico Nacional, Av. IPN UPALM Edif. 7 P.B., Zacatenco, México D.F. 07738, Mexico

[§]Universidad Autónoma Metropolitana, Iztapalapa, Av. San Rafael Atlixco No. 186, Col. Vicentina, CP 09340, México D.F., Mexico

[∥]Laboratoire de Physique et Etude des Matériaux (LPEM), Université Pierre et Marie Curie and ESPCI, 10 Rue Vauquelin, 75231 Paris cedex 05, France

**ABSTRACT:** Maya Blue-like pigments were prepared by two routes using a palygorskite from the Maya region. Synthetic indigo was used as a dye in one case, while the other used the añil plant (*Indigofera suffructicosa*). Both synthetic and natural Maya Blue pigments were aged and characterized in order to clarify the interaction of the dye-palygorskite. Natural and synthetic fresh Maya Blue pigments were very different; the synthetic ones obviously stabilized the indigo molecule probably at the clay surface and may be in the grooves, but the natural ones stabilized indoxyl molecules in the tunnels and over time oxidized to indigo. The presence of indigo, originating from the añil plant, into palygorskite tunnels was evidenced in aged natural pigments by $^{29}$Si, $^{27}$Al, $^{13}$C, and $^{129}$Xe NMR. The persistence of color was evaluated as a function of leaching dye under acidic conditions.

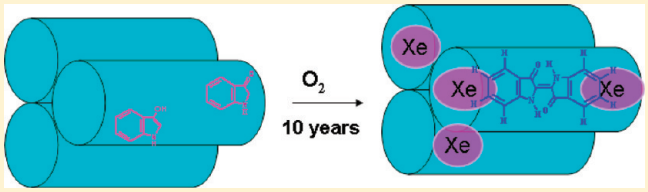


## INTRODUCTION

The famous pre-Columbian Maya Blue (MB) pigment has been the subject of many research papers.[1−4] Most research focused on explaining the extreme stability of this hybrid organic/inorganic pigment, which is present in mural paintings in Mayan ceremonial sites in the Yucatan, as well as in many ceramic pieces. More recently, it was also identified in the large monolith, *Tlaltecuhtli*,[5,6] which represents the Aztec Earth god.

In the MB pigment, the host is the fibrous palygorskite clay, and the guest is the indigo molecule. Palygorskite is a fibrous hydrated T−O−T phyllosilicate built by continuous two-dimensional tetrahedral sheets of $Si_2O_5$. In the palygorskite structure (Figure 1 right), narrow strips or ribbons of 2:1 layers are linked stepwise at the corners. One ribbon is linked to the other by inversion of the direction of the apical oxygen atoms of $SiO_4$ tetrahedrons in such a way that the structure can be regarded as an elongated rectangular box consisting of continuous 2:1 layers, which are attached to the nearest boxes at their elongated corner edges. Thus, the absence of the silicate layers on the elongated sides of the boxes leads to the formation of tunnels with a cross-section sized 3.7 × 6.4 Å (for hydrated clay). The octahedral sheet is discontinuous; some octahedral ions (mainly $Mg^{2+}$) are exposed at the edges and hold the bound water molecules. The palygorskite is generally represented by the formula $Si_8(Mg_2Al_2)O_{20}(OH)_2(OH_2)_4{\cdot}4H_2O$.[7−9] Composition can vary depending of the source; for instance the Palygorskite from Yucatán, Mexico, is represented by the formula $Si_{7.61}(Mg_{2.19}Al_{1.93}Fe_{0.23}Ti_{0.03})O_{20}(OH)_2Ca_{0.15}Na_{0.17}K_{0.11}(OH_2)_4{\cdot}4H_2O$.[10] Figure 1 left shows a schematic cross-section of the palygorskite structure, perpendicular to the tunnel's direction. One can see the three different configurations of octahedral sites as M1, M2, and M3 in the structure. The M1 sites have a *trans*-OH configuration. The M2, occupied by $Al^{3+}$, sites have a *cis*-OH configuration with a pair of OH ions being shared between two adjacent octahedra. The M3 sites, occupied by $Mg^{2+}$, have two water ligands and are present at the edges of the octahedral ribbons.

Indigo is an organic dye, $C_{16}H_{10}N_2O_2$ (size 4.8 Å to 12.3 Å), with a quasi-planar structure (Figure 2a). On Figure 2b is provided the structural formula of the indoxyl, a precursor of indigo.

The host−guest interaction is claimed to be at the origin of great stability of the pigment, but the location of indigo in MB remains controversial. Depending on the authors, indigo lies in grooves at the surface of the clay fibers,[3,11,12] entering the internal tunnels and replacing the zeolitic water,[13−15] or does not enter the clay but stays at the tunnel entrances.[16,17]

The proposed models for the interaction that anchors indigo to palygorskite include (i) formation of hydrogen bonds between the C═O and N−H groups with edge silanol units of the clay, (ii) formation of hydrogen bonds between indigo molecules and structural OH groups, (iii) hydrogen bond formation between indigo carbonyls and structural $H_2O$, (iv) direct bonding between the clay octahedral cations and the dye molecules without $H_2O$, and (v) specific bonding to Al substituted Si sites in tetrahedral centers.[14,16,18] Finally, for some authors,

**Received:** August 8, 2011
**Revised:** January 23, 2012
**Published:** January 24, 2012

  

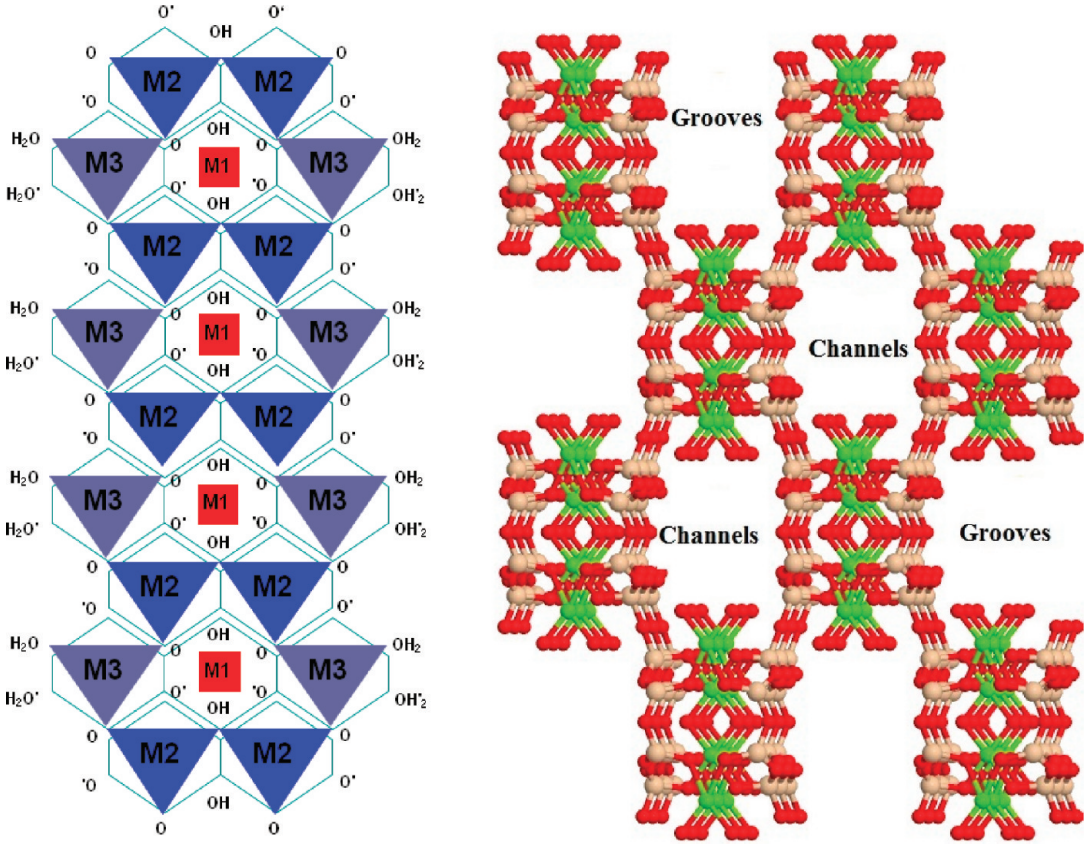


**Figure 1.** Structure of palygorskite clay (right) showing the tunnels where indigo dye could be hosted; gray = silicon, red = oxygen, and green = magnesium or aluminum. Projection on directions a and b (left) showing the octahedral sites. In this projection O′, OH′, and $H_2O$′ form the bottom triangles while O, OH, and $H_2O$ fit in the top triangles of the octahedral. Adapted with permission from ref 7. Copyright 2009 Mineralogical Society of America.

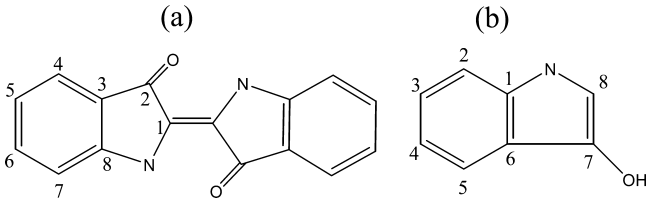


**Figure 2.** Structural formula for indigo (a) and indoxyl (b) molecules.

the chemical stability in MB depends more on steric shielding than on the strength of chemical bonding.[19] Molecular modeling[15] suggests that indigo molecules diffuse into the tunnels and eventually reach several stable sites where they are trapped. Further, theoretical calculations suggested that the most likely association between the organic dye and the inorganic clay involves $Al^{3+}$ cations, exposed at the edge of the clay tunnels, and the carbonyl group of the dye adsorbed on the surface.[20]

Among the numerous papers published on MB, very few used original samples taken from Mayan sites. This fact is comprehensible because of the difficulty in obtaining a considerable amount of archeological pigment for examination through physicochemical and spectroscopic techniques. Instead, most papers reported results obtained with fresh MB pigments prepared using palygorskite clay collected from different sources and with indigo provided by commercial chemical companies. The MB pigments can be prepared using leaves of the añil plant,[21−23] which is the source of indigo that the Maya used.

The samples prepared from indigo and palygorskite have been considered to be part of the family of pigments called Maya Blue-like pigments. The other part of the family is a pigment series where other aluminiosilicates (mainly sepiolite and silicalite) host synthetic indigo molecules.[24,25] The Maya Blue-like stable pigments are now available within a wide variety of colors and hues; these pigments are commercially available. In fact, many other hybrid pigments have been prepared, inspired by the Mayan technique.[26,27]

The mystery regarding the stability of MB has not been resolved. As mentioned above, several studies are not in agreement, and the synthetic samples may not match exactly with the original pigment. In order to discard or confirm the hypothesis that indigo molecules are stabilized inside the tunnels of the clay, many experimental indirect information about the tunnels of clays has been carried out,[4] but the inner MB should be directly examined. This observation has been achieved only virtually. These studies attempt to be convincing, but the materials simulated could be far from the real Mayan world. Thus, we have started this work with the goal of visiting the interior of tunnels of the MB pigments prepared by a protocol believed to be close to those used by the Mayan people. To spy the interior of the MB tunnels is possible using nuclear magnetic resonance (NMR) of $^{29}Si$, $^{27}Al$, $^{13}C$, and $^{129}Xe$ of adsorbed xenon. Xenon has a kinetic diameter of 4.4 Å and has very high polarizability; therefore, its diffusion in the direction of the length of the tunnels of palygorskite is possible. $^{129}Xe$ NMR has proved to be a sensitive technique used to characterize the different porous media in detail.[28−33] Further, we have aged the


dx.doi.org/10.1021/jp207602m | J. Phys. Chem. C 2012, 116, 4556−4563

samples and the evolution of the nature host−guest interaction was followed, in particular by $^{13}C$ NMR.

## EXPERIMENTAL PROCEDURE

**Materials.** *Traditional Maya Blue.* Maya Blue samples were prepared according to the traditional method, as reported by Reyes-Valerio.[34] Briefly, in 100 mL of distilled water, 1.5 g of palygorskite clay (from Yucatán, Mexico) and 5 g of fresh washed leaves from the añil plant (Figure 3; *Indigofera suffructicosa* from Niltepec, Oaxaca, Mexico) were placed in contact for 18 h at room temperature. The añil leaves were removed, and the suspension was stirred vigorously for 20 min. The suspension settled for 1 h and was finally filtered; the filtered solid was dried at 180 °C overnight, obtaining a bluish solid.

**Figure 3.** Añil (*Indigofera suffructicosa*) plant, containing the indigo dye used to prepare Maya Blue-like pigments.

*Synthetic Maya Blue.* MB pigment was prepared following the procedure described in many previous studies.[3] A mixture of palygorskite clay from the Yucatán and synthetic indigo from Aldrich were finely ground and heated to 180 °C for 24 h. This procedure is the most common one used to prepare MB-like pigments. It is worth noting that the indigo is not soluble in water. In order to elucidate the role of solvent as a possible determinant factor of indigo diffusion and stabilization on clay, another sample was prepared with the same ratio of indigo/clay but with indigo dissolved in dimethyl sulphoxide (DMSO), provided by Aldrich. The color of MB pigments emerged from these two preparations, using indigo, was enhanced blue.

Table 1 summarizes the synthesis conditions of the samples considered in this study. The corresponding sample codes and the number of water and indigo molecules per gram of pigment were determined by chemical analyses. It was assumed that the total amount of carbon is retained as indigo. Two traditional Maya Blue samples were prepared by varying the ratio of añil/palygorskite. For comparison purposes, the synthetic Maya Blue pigment was prepared by maintaining the same total amount of carbon that was found in one of the two traditional Maya Blue samples considered.

*Accelerated Aging.* Samples were treated to simulate aging. Samples were placed in an Accelerated Weathering Tester from the Q Panel Company QUV. The temperature was maintained at 45 to 50 °C for 16 h under UV exposure and a relative humidity of 20 to 30%, followed by 8 h at 45 to 50 °C under 80 to 100% relative humidity without UV exposure. This cycle was repeated for 200 days, which is equivalent to 10 years in real time. The code of aged samples includes the prefix A instead of F, which is used for the fresh samples.

**Characterization.** Samples were characterized by NMR of $^{29}Si$, $^{27}Al$, $^{13}C$, and $^{129}Xe$ of adsorbed xenon. Solid-state $^{27}Al$ and $^{29}Si$ NMR single excitation spectra were acquired on a Bruker Avance 400 spectrometer. $^{29}Si$ NMR spectra were acquired at 79.46 MHz using the combined techniques of magic angle spinning (MAS) and proton dipolar decoupling (HPDEC). Direct-pulsed NMR excitation was used throughout the experiment, employing 90° pulses (3 $\mu$s) with a pulse repetition time of 40 s. Powdered samples were packed in zirconia rotors. The spinning rate was 5 kHz, and the chemical shifts were referenced to TMS.

The $^{27}Al$ MAS NMR spectra were acquired under MAS conditions operating the spectrometer at a frequency of 104.2 MHz. Short single pulses ($\pi/12$) were used. The samples were spun

**Table 1. Characteristic of the Samples**

| sample code | components (precursors) | estimated number of indigo molecules per gram of pigment[ab] | indigo (wt %) in sample | estimated number of water molecules per gram of pigment[cd] |
|---|---|---|---|---|
| F-NMB1 | palygorskite and fresh leaves of añil | $2.987 \times 10^{19}$ | 1.3 | $3.13 \times 10^{21}$ |
| F-NMB2 | palygorskite and dried leaves of añil | $5.974 \times 10^{19}$ | 2.6 | $3.02 \times 10^{21}$ |
| F-SMB1 | palygorskite and indigo from Aldrich | $5.974 \times 10^{19}$ | 2.6 | $2.41 \times 10^{21}$ |
| F-SMB2 | palygorskite and indigo from Aldrich diluted in DMSO | $5.974 \times 10^{19}$ | 2.6 | $2.53 \times 10^{21}$ |
| F-PAL | palygorskite | | | $2.95 \times 10^{21}$ |
| A-NMB1 | palygorskite and fresh leaves of añil after aging | $2.987 \times 10^{19}$ | 1.3 | $2.39 \times 10^{21}$ |
| A-NMB2 | palygorskite and dried leaves of añil after aging | $5.974 \times 10^{19}$ | 2.6 | $2.24 \times 10^{21}$ |
| A-SMB1 | palygorskite and indigo from Aldrich after aging | $5.974 \times 10^{19}$ | 2.6 | $2.46 \times 10^{21}$ |
| A-SMB2 | palygorskite and indigo from Aldrich diluted in DMSO after aging | $5.974 \times 10^{19}$ | 2.6 | $2.59 \times 10^{21}$ |
| A-PAL | palygorskite after aging | | | $2.51 \times 10^{21}$ |
| A-SMB1- ac | palygorskite and indigo from Aldrich after aging and acid treatment | $2.920 \times 10^{19}$ | 1.26 | |
| A-NMB2-ac | palygorskite and dried leaves of añil after aging and acid treatment | $4.986 \times 10^{19}$ | 2.2 | |

[a]As determined by chemical analysis. [b]Error associated ±5%. [c]As determined by thermal analysis. [d]Error associated ±3%.


dx.doi.org/10.1021/jp207602m | J. Phys. Chem. C 2012, 116, 4556−4563

at 10 kHz, and the chemical shifts were referenced to an aqueous 1 M $AlCl_3$ solution.

The $^{13}C$ CP/MAS NMR spectra were acquired at a frequency of 75.422 MHz at a spinning rate of 5 kHz. Typical $^{13}C$ CP/MAS NMR conditions for $^{1}H-^{13}C$ polarization experiment used a $\pi/2$ pulse of 4 $\mu$s, contact time of 1 ms, delay time of 5 s, and at least 80 000 scans. Chemical shifts were referenced to a solid shift at 38.2 ppm relative to TMS.

Xenon gas (Praxair, 99.999%) was used for the $^{129}Xe$ NMR measurements. For these experiments, the sample was placed in a NMR tube equipped with Young valves through which the xenon gas was equilibrated with the sample at 20 °C under different pressures. Prior to xenon loading, samples were dehydrated by gradual heating up to 80 °C under vacuum ($1.33 \times 10^{-4}$ kPa). These soft conditions were used in order to avoid any change in the interaction of the clay–dye. Colors of pigments before and after vacuum treatment were similar, assuming that desorption of the dye did not occur. The $^{129}Xe$ NMR spectra were recorded at 20 °C while operating the spectrometer at 111.23 MHz. Single excitation pulses were used, and at least 5000 scans were collected with a delay time of 2 s. The chemical shift was referenced to xenon gas extrapolated to zero pressure.

**Dye Desorption.** Maya Blue-like pigments were tested for dye desorption by refluxing the samples in aqueous 5 M $HNO_3$ . The samples were acid treated several times. Solids and liquids were separated by centrifugation, and the desorbed dye was quantified in solutions by UV–vis spectroscopy; analysis was performed by interpolating the intensities measured in a calibration curve that was previously created.

## RESULTS AND DISCUSSION

Fresh synthetic MB pigments (F-SMB) were enhanced blue colored. In contrast, the natural fresh MB samples (F-NMB) were only pale blue, and with aging, the blue was considerably enhanced.

Figure 4 displays the $^{29}Si$ spectra of both synthetic and natural MB samples. Spectra of four fresh pigments (Figure 4a)

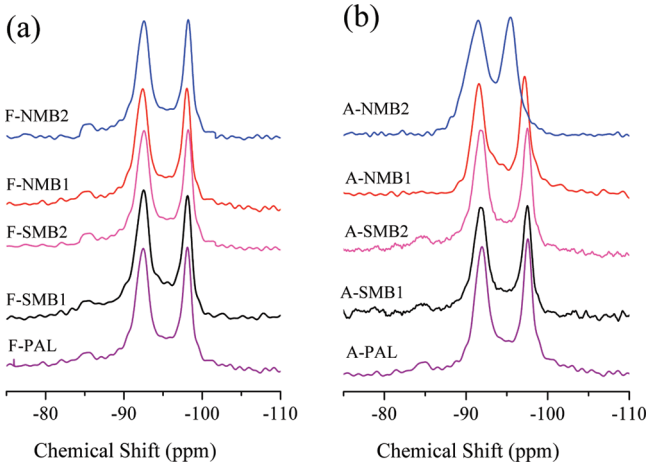


**Figure 4.** $^{29}Si$ MAS NMR spectra of fresh (a) and aged (b) Maya Blue-like pigments.

are very similar to the spectrum of free-dye palygorskite (F-PAL). The spectrum shows three resonance peaks, and two are very intense; the first peak at −97.5 ppm is assigned to the edge Si nuclei. The second intense resonance at −93.0 ppm is due to the center silicon nuclei. Lastly, a small peak is observed close to −85 ppm, which is due to $Q^2$(Si–OH)Si sites, located at the edge of the ribbons at the crystal edges or defects.[35,36] All three resonances were observed in fresh pigments with a similar width and at the same position, suggesting that the dye molecules are not strongly interacting with the silicon atoms. Because of the propositions regarding the dye–clay interactions, one could expect that the aluminum atoms play an important role as receptors of dye. The $^{27}Al$ MAS NMR spectra, shown in Figure 5a, however, do not support this hypothesis because the

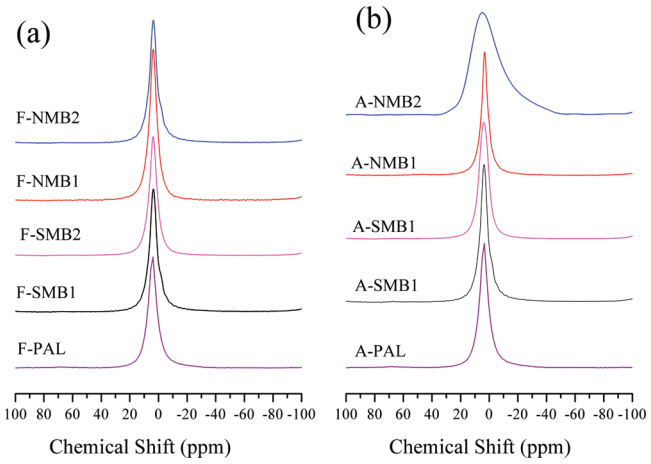


**Figure 5.** $^{27}Al$ MAS NMR spectra of fresh (a) and aged (b) Maya Blue-like pigments.

spectra of the four fresh pigments are very similar to the spectrum of palygorskite, which presents an isotropic signal close to 0 ppm due to aluminum 6-fold coordinated in an oxygen environment.[8,37] These results suggest that in fresh samples, the clay–dye interaction does not occur directly with Al or Si, which is reasonable because of the low reactivity of silicons in clay and the internal position (M2 sites) of aluminum. It should be concluded that the clay–dye interaction in fresh samples should be only a physical adsorption at the surface of the clay, in agreement with previous works supported by TEM, SEM, thermal analysis, and theoretical studies.[11,27]

With aging, $^{27}Al$ and $^{29}Si$ NMR spectra of free-dye palygorskite clay (A-PAL) remain unchanged, supporting that water remains adsorbed close to aluminum. Likewise, the three peaks in the $^{29}Si$ NMR spectra of both fresh and aged synthetic SMB samples are roughly identical (Figure 4a,b, respectively). In the case of the dye in aged pigments, A-SMB indigo does not interact with the silicon layers. $^{27}Al$ NMR spectra of samples SMB1 and SMB2, before and after aging, also remained similar (Figure 5). This feature supports that in synthetic MB pigments, the interaction of indigo and palygorskite does not occur through aluminum atoms. A symmetric and narrow peak of $^{27}Al$ resonance in this pigment suggests that structural water is adsorbed close to aluminum and prevents the approach of the dye molecules.

On the contrary, the $^{29}Si$ MAS NMR spectra of natural NMB pigments changed with aging and revealed an evolution of the dye–clay interaction. In aged NMB1 and NMB2 samples, the low intense peak at −85 ppm faded out completely; only two intense resonance peaks are observed reaching the same integrated intensity. Further, the chemical shifts of the signals in the spectrum of sample loaded with the higher amount of dye (NMB2) are shifted 3 ppm to higher chemical shift values, and they are roughly 200 Hz broader than those observed for fresh


dx.doi.org/10.1021/jp207602m | J. Phys. Chem. C 2012, 116, 4556–4563

pigments. This is the first evidence that indigo is inside the clay tunnels. The incorporation of indigo into tunnels of palygorskite has to correlate to the elimination of water molecules. The absence of the resonance at −85 ppm was previously related to dehydration and decomposition of the ribbons of clay.[38] In addition, the $^{29}$Si NMR spectra are sensitive to desorption of zeolitic water molecules,[35] then also to the adsorption of other species. This explanation is also supported by the $^{27}$Al MAS NMR spectra, (Figure 5a,b), which show that the narrow and symmetric peak in the spectrum of sample F-NMB2 becomes significantly broader and asymmetric in the spectrum of A-NMB2. This can be explained because of the exchange of some water molecules close to the aluminum atoms with dye molecules, maintaining the 6-fold coordination around aluminum but changing some of its symmetry. The loss of water was confirmed by thermal analysis, as seen in Table 1. These results could be interpreted as a folding of clay but this hypothesis is discarded because C. Dejoie et al. analyzed original Maya Blue pigments and reported that indigo prevents the clay folding.[19]

For the sake of conciseness, only some $^{129}$Xe NMR spectra of xenon adsorbed at different pressures on the F-NMB1 sample are presented in Figure 6. All spectra show a low signal/noise ratio due to the low amount of adsorbed xenon.

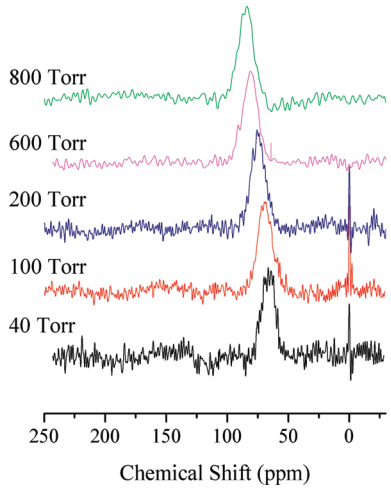


**Figure 6.** $^{129}$Xe NMR spectra of xenon adsorbed at indicated pressures on F-NMB1 sample.

All fresh and aged samples, including the free-dye palygorskite, presented similar spectra, with a single isotropic signal whose chemical shift increases with the amount of adsorbed xenon (Figures 7 and 8) and fit very well to linear relationships as follows:[29,33,39]

$$\delta(\rho) = \delta_0 + \delta_S + \delta_1\rho \qquad ([1])$$

where $\delta_0$ is the reference, and $\delta_s$ is the term due to the interaction between xenon and the wall of the clay tunnels. More precisely, $\delta_S$ is related to the mean free path of a Xe atom within a pore because it depends not only on the dimensions of the pores but also on the ease of diffusion inside the solid crystallites.[33,39] Typically, the smaller the value of $\delta_S$, the larger the pore size.[33,39,40] This dependence was first expressed for zeolites and was later validated for many other types of microporous materials, including two-dimensional network structures such as clays.[41−43] The $\delta_S$ values are indeed the same, 66.5 ± 1 ppm, for the four

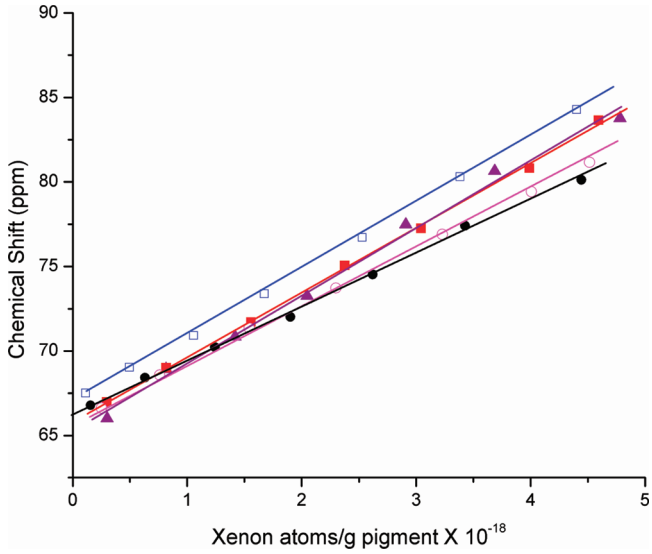


**Figure 7.** $^{129}$Xe chemical shift as a function of concentration of xenon in (▲) F-PAL, (■) F-NMB1, (□) F-NMB2, (●) F-SMB1, and (○) F-SMB2. The error associated to the value of chemical shift is ±1 ppm.

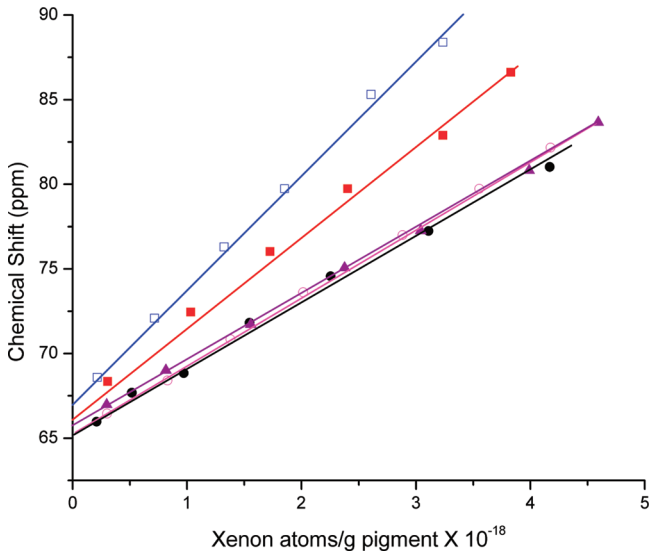


**Figure 8.** $^{129}$Xe chemical shift as a function of concentration of xenon in (▲) A-PAL, (■) A-NMB1, (□) A-NMB2, (●) A-SMB1, and (○) A-SMB2. The error associated to the value of chemical shift is ±1 ppm.

fresh MB pigments, as well as for the palygorskite without dye (F-PAL). This value of $\delta_S$ agrees with the pore size of palygorskite. $\delta_1$ is the coefficient describing the effects of xenon−xenon collisions, and $\rho$ is the xenon density (atoms per gram of pigment). The slope of lines $\delta = f(\rho)$ is related to the free porous volume. The slopes of the two lines corresponding to both fresh natural pigments (F-NMB1 and F-NMB2) and for the line for F-PAL are the same. The same $\delta_S$ and $\delta_1$ means that the three materials have similar pore sizes and free volumes, and the adsorbed species are only located at the external surface of the clay as supported by $^{29}$Si and $^{27}$Al NMR results. Additionally, the slopes of the lines for the two synthetic pigments, F-SMB1 (preparation without solvent) and F-SMB2 (preparation in DMSO), are very close and slightly lower than those of palygorskite. This fact is due to the lower content of water in


dx.doi.org/10.1021/jp207602m | J. Phys. Chem. C 2012, 116, 4556−4563

these pigments as determined by thermal analysis (Table 1). The difference in the content of water is originated by the preparation method. In conclusion, the previous results by $^{129}$Xe NMR confirm those obtained with $^{29}$Si and $^{27}$Al NMR: dye does not diffuse into the tunnels of synthetic fresh pigments, whatever their preparation.

With aging, the variations of the chemical shifts against the amount of xenon (Figure 8) are more interesting. Because the PAL samples do not contain any organic molecules, the slight difference of the slopes between F-PAL and A-PAL is only due to the small decrease in the water concentration with aging (Table 1). The variation of $\delta(\rho)$ in both synthetic MB pigments, A-SMB1 and A-SMB2, are identical to that obtained for A-PAL. Because these three samples contain a similar content of water, it is concluded that the indigo is not inside the tunnel of the aged synthetic samples. Whatever the preparation (free solvent or in DMSO), using pure indigo leads to a strong stabilization of dye at the surface of clay, inhibiting its diffusion into the tunnels.

On the contrary, with aging, an increase of the $\delta_1$ slopes for A-NMB1 and A-NMB2 was observed, as compared with those of the fresh samples. Further, the higher the concentration of dye, the higher the slope. This result can be interpreted as a presence of indigo inside the tunnels and grooves as a function of its concentration. It is worth noting that the $\delta_S$ value is the same and is within the experimental error for all natural pigments, fresh and aged, which suggests that some of the tunnels are blocked by indigo and others are dye-free. The diffusion of dye into the tunnels of the A-NMB2 sample may be so important that the zeolitic water is displaced to favor the stabilization of dye.

Regarding the A-NMB2 sample, the previous results must be relevant to explain the persistence of the color in Maya pigments. In this context, curves displayed in Figure 9 show the

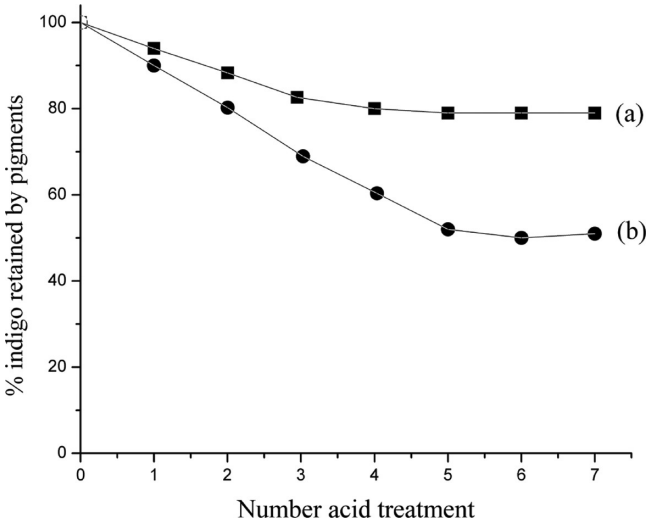


**Figure 9.** Percent indigo retained by the pigments after consecutive acid treatments. (a) A-NMB2 and (b) A-SMB1.

amount of dye retained in the solids after leaching under acidic conditions. After seven consecutive acid attacks on A-NMB2, the sample (A-NMB2-ac, Table 1) leached approximately 20% of dye. In contrast, the synthetic A-SMB1 pigment releases a high percentage, up to 50% of dye, after five acid treatments (A-SMB1-ac, Table 1). The dye more accessible, i.e., the dye present at the external surface of the clay, is easily attacked by acid. Thus, the stabilization of dye at the surface of the synthetic pigment implies a vulnerability of this pigment to acid attacks.

After acid treatment, $^{129}$Xe NMR experiments were carried out with A-NMB2-ac and A-SMB1-ac. The plots of chemical shift versus xenon amounts are presented in Figure 10. In order

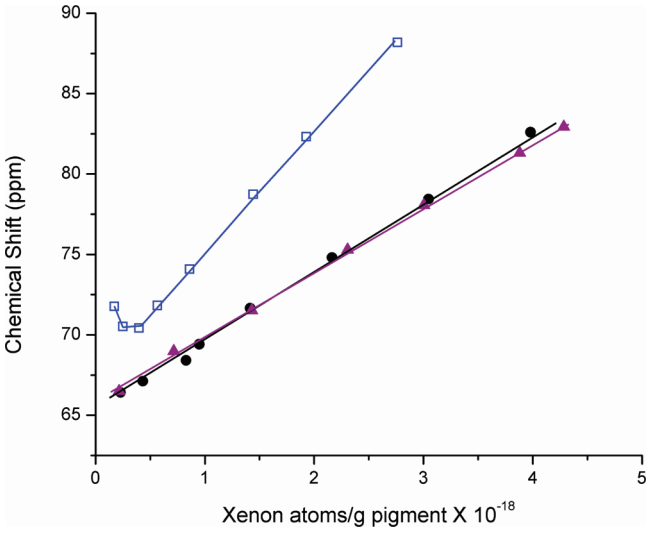


**Figure 10.** $^{129}$Xe chemical shift as a function of concentration of xenon in samples after acid treatment. (▲) A-PAL-ac, (□) A-NMB2-ac, and (●) A-SMB1-ac.

to have a reference material, the curve for palygorskite clay, acid treated in the same way that the pigments were, is also included (A-PAL-ac). Within the experimental errors, the plots for A-SMB1-ac, A-PAL, and A-PAL-ac coincide. This result confirms the assumption above, suggesting that aging does not induce the penetration of indigo into the tunnels of the synthetic samples.

Alternatively, the curve for acid treated A-NMB2-ac presents a slight minimum at a low concentration of xenon. A linear behavior is observed at higher xenon loading with a slope slightly greater than that for the sample before acid treatment. The value of $\delta$ determined by extrapolation of the line for zero concentration is equal to $\delta_S$. These results show that the free volume of the A-NMB2 sample is slightly lowered by the acid treatment, creating a few strong adsorption sites, likely cations removed from the framework.[28,33] These variations, however, are relatively weak and are the consequence of a very strong acid treatment. It is confirmed that the stability of the A-NMB2 sample is similar to the stability of the original Maya Blue pigments.

The different behaviors of MB pigments prepared from synthetic indigo and from añil leaves remain questionable. It should be emphasized that indigo is water insoluble. Indigo from leaves in aqueous solution should precipitate on the surface of the clay without any diffusion in the pores, according to the results obtained with synthetic indigo. However, añil leaves also provide indoxyl and indican (easily hydrolyzed to indoxyl), which are both soluble in water and smaller than indigo. These molecules can be adsorbed on the clay surface and diffuse much more easily into the pores; they are oxidized under atmospheric oxygen during aging to give indigo. In this sense, $^{13}$C CP/MAS NMR spectra displayed in Figure 11


dx.doi.org/10.1021/jp207602m | J. Phys. Chem. C 2012, 116, 4556–4563

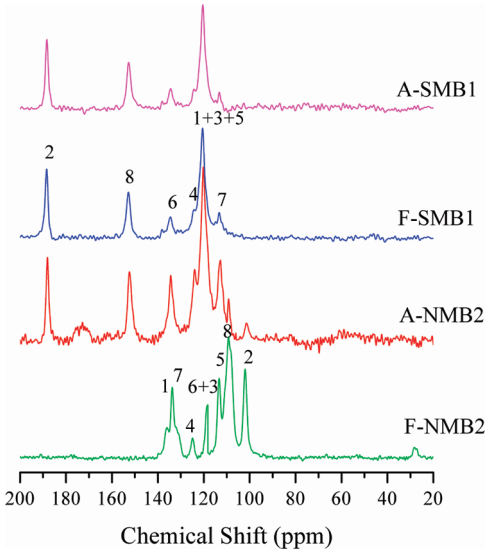


**Figure 11.** Solid-state $^{13}C$ CP/MAS NMR spectra of fresh and aged MB pigments.

confirm this hypothesis. Spectra of fresh, synthetic, and natural MB pigments are very different. NMR peaks of the spectrum of F-SMB1 were assigned to the indigo molecule (peaks labeled according to carbons numbered in Figure 2a). In contrast, the spectrum of F-NMB2 matches with the indoxyl molecule, where the numbering of peaks corresponds to the numbering of carbons of Figure 2b.

With aging, the spectrum of synthetic pigment remains unaltered; the indigo molecules were stable on the palygorskite over the time. The presence of indigo is also evident (intense peaks at 112, 120, 123, 124, 142, and 188 ppm) in the aged natural pigment (A-NMB2). Clearly, the indoxyl was oxidized to indigo. A minor amount of indoxyl (peaks at 101 and 109 ppm) remained without being oxidized. This explanation has been previously suggested[12,44] and is in complete agreement with our results.

These results explain the variations above-mentioned about the color differences between the natural MB samples, before and after aging. For example, F-NMB2 is slightly bluish, while A-NMB2 became enhanced blue.

The case of A-NMB1 may seem surprising, the variation in $\delta(\rho)$ seems to contradict the $^{29}Si$ and $^{27}Al$ NMR spectra, practically unchanged. In fact, according to the theoretical conclusions of C. Dejoie et al,[19] indigo populates successively the very stable sites at the tip fibers, then the groove sites, and finally the tunnels. Sample A-NMB1 having a concentration of adsorbate relatively lower than A-NMB2, the change in slope of $\delta(\rho)$ may be due exclusively to the filling of the grooves, which have almost the same dimensions as that the tunnels, but this does not influence the silicon and aluminum sites in the tunnels.

## CONCLUSIONS

This work aimed to understand the interaction between indigo dye and palygorskite clay from the Maya region. The dye was added to clay three different ways: (i) the traditional Mayan technique, mixing the palygorskite with aqueous solution of leaves of the añil plant; (ii) the synthetic recurrent method, mixing palygorskite and synthetic indigo finely ground and heated to 180 °C; and (iii) a variant of the synthetic method mixing palygorskite and synthetic indigo dissolved in DMSO.

NMR spectra of $^{29}Si$, $^{27}Al$, and adsorbed xenon $^{129}Xe$ show that only the sample prepared by the traditional technique contains indigo inside the tunnels of palygorskite. With samples prepared from synthetic indigo, an interaction between indigo and the external surface of the clay is favored.

The acid treatment of samples after aging provides evidence for the chemical resistance of pigments prepared from the traditional technique when compared to the synthetic samples. This behavior agrees with the distribution of dye in the samples, as elucidated by NMR.

The indigo dye from añil leaves is water insoluble; therefore, it should be deposited on the external surface of clay without any diffusion in the pores, according to the results relative to the synthetic samples. The presented results, particularly the $^{13}C$ NMR spectra, prove that some smaller precursors of indigo, such as indoxyl, should be adsorbed on the clay surface and diffuse more easily into the pores; they are ultimately oxidized under atmospheric oxygen to provide indigo.

## AUTHOR INFORMATION

### Corresponding Author

*Phone: +52 (55) 5622 4640. Fax: +52 (55) 5616 1371. E-mail: lima@iim.unam.mx.

### Notes

The authors declare no competing financial interest.

## ACKNOWLEDGMENTS

Thanks are due to CONACYT for Grants 128299 and 101319 and PAPIIT-UNAM IN107110. We gratefully acknowledge A. Tejeda, G. Cedillo, M. Canseco, and E. Fregoso for the technical help.

## REFERENCES

(1) Merwin, H. E. In *Chemical Analysis of Pigments in Temple of the Warriors at Chichén-Itzá, Yucatán*; Morris, E. H., Charlot, J., Morris, A. A., Eds.; Carnegie Inst., Washington DC, 1931; pp 355−356.
(2) Shepard, A. O. *Am. Antiq.* **1962**, *27*, 565−566.
(3) Van Olphen, H. *Science* **1967**, *154*, 645−646.
(4) Sanchez del Río, M.; Domenech, A.; Domenech-Carbo, M. T.; Vazquez de Agredos Pascual, M. L.; Suarez, M.; García-Romero, E. *Developments in Clay Science*; Singer, A., Galan, E., Eds.; Elsevier: Amsterdam, The Netherlands, **2011**; Vol. 3, Chapter 18, pp 453−481
(5) Barajas, M.; Lima, E.; Lara, V.; Vázquez-Negrete, J.; Barragán, C.; Malváez, C.; Bosch, P. *J. Archaeol. Sci.* **2009**, *36*, 2244−2252.
(6) Barajas, M.; Bosch, P.; Malváez, C.; Barragán, C.; Lima, E. *J. Archaeol. Sci.* **2010**, *37*, 2881−2886.
(7) Chryssikos, G. D.; Gionis, V.; Kacandes, G. H.; Stathopoulou, E. T.; Suárez, M.; García-Romero, E.; Sánchez Del Río, M. *Am. Mineral.* **2009**, *94*, 200−203.
(8) García-Romero1, E.; Suárez, M. *Clays Clay Miner.* **2010**, *58*, 1−20.
(9) Güven, N.; d'Espinose de la Caillerie, J.-B.; Fripiat, J. J. *Clays Clay Miner.* **1992**, *40*, 457−461.
(10) De Pablo-Galán, L. *Rev. Mex. Cienc. Geol.* **1996**, *13*, 94−103.
(11) Polette-Niewold, L. A.; Manciu, F. S.; Torres, B.; Alvarado, M.; Chianelli, R. R. *J. Inorg. Biochem.* **2007**, *101*, 1958−1973.
(12) Chiari, G.; Giustetto, R.; Druzik, J.; Doehne, E.; Ricchiardi, G. *Appl. Phys. A: Mater. Sci. Process.* **2008**, *90*, 3−7.
(13) Kleber, R.; Masschelein-Kleiner, R.; Thissen. *Stud. Conserv.* **1967**, *12*, 41−55.
(14) Chiari, G.; Giustetto, R.; Ricchiardi, G. *Eur. J. Miner.* **2003**, *15*, 21−33.
(15) Fois, E.; Gamba, A.; Tilocca, A. *Microporous Mesosporous Mater.* **2003**, *57*, 263−272.

(16) Hubbard, B.; Kuang, W.; Moser, A.; Facey, G. A.; Detellier, C. *Clays Clay Miner.* **2003**, *51*, 318−326.
(17) Sánchez del Rio, M.; Boccaleri, E.; Milanesio, M.; Croce, G.; van Beek, W.; Tsiantos, C.; Chyssikos, G. D.; Gionis, V.; Kacandes, G. H.; Suarez, M.; Garcia-Romero, E. *J. Mater. Sci.* **2009**, *44*, 5524−5536.
(18) Giustetto, R.; Llabres Xamena, F. X.; Ricchiardi, G.; Bordiga, S.; Damin, A.; Gobetto, R.; Chierotti, M. R. *J. Phys. Chem. B* **2005**, *109*, 19360−19368.
(19) Dejoie, C.; Dooryhée, E.; Martinetto, P.; Blanc, S.; Bordat, P.; Brown, R.; Porcher, F.; Sanchez del Rio, M.; Strobel, P.; Anne, M.; Van Elslande, E.; Walter, P. Revisiting Maya Blue and Designing Hybrid Pigments by Archaeomimetism, 2010. http://hal.archives-ouvertes.fr/hal-00495128/fr; arXiv:10070818.
(20) Tilocca, A.; Fois, E. *J. Phys. Chem. C* **2009**, *113*, 8683−8687.
(21) Doménech, A.; Doménech, M. T.; Vázquez, M. L. *J. Solid State Electrochem.* **2007**, *11*, 1335−1346.
(22) Sánchez del Río, M.; Martinetto, P.; Reyes-Valerio, C.; Déoryhee, E.; Suárez, M. *Archaeometry* **2006**, *48*, 115−130.
(23) Littmann, E. R. *Am. Antiq.* **1980**, *45*, 87−100.
(24) Doménech, A.; Doménech-Carbó, M. T.; del Río Sánchez, M.; Goberna, S.; Lima, E. *J. Phys. Chem. C* **2009**, *113*, 12118−12131.
(25) Dejoie, C.; Martinetto, P.; Dooryhe, E.; Strobel, P.; Blanc, S.; Bordat, P.; Brown, R.; Porcher, F.; Sanchez del Rio, M.; Anne, M. *ACS Appl. Mater. Interfaces* **2010**, *2*, 2308−2316.
(26) Lima, E.; Bosch, P.; Loera, S.; Ibarra, I.; Laguna, H.; Lara, V. *Appl. Clay Sci.* **2009**, *42*, 478−482.
(27) Laguna, H.; Loera, S.; Ibarra, I.; Lima, E.; Vera, M.; Lara, V. *Microporous Mesoporous Mater.* **2007**, *98*, 234−241.
(28) Fraissard, J.; Ito, T. *Zeolites* **1988**, *8*, 350−361.
(29) Springuel-Huet, M. A.; Fraissard, J. *Chem. Phys. Lett.* **1989**, *154*, 229−302.
(30) Romanenko, K. V.; Py, X.; d'Espinose de Lacaillerie, J. B.; Lapina, O. B.; Fraissard, J. *J. Phys. Chem. B* **2006**, *110*, 3055−3060.
(31) De Menorval, L. C.; Raftery, D.; Liu, S. B.; Takegoshi, K.; Ryoo, R.; Pines, A. *J. Phys. Chem.* **1990**, *94*, 27−31.
(32) Ito, T.; Fraissard, J. *J. Chem. Phys.* **1982**, *76*, 5225−5229.
(33) Bonardet, J.; Gédeon, A.; Springuel-Huet, M.-A.; Fraissard, J. In *Molecular Sieves, Chracterization II*; Karge, H. G., Weitkamp, J., Eds.; Springer: New York, 2007; pp 155−248,
(34) Reyes Valerio, C. *De Bonampak Al Templo Mayor*; Siglo XXI: México, 1993.
(35) Kuang, W.; Facey, G. A.; Detellier, K. *Clays Clay Miner.* **2004**, *52*, 635−642.
(36) d'Espinose de la Caillerie, J.-B.; Fripiat, J. J. *Clays Clay Miner.* **1994**, *29*, 313−318.
(37) Lippmaa, E.; Magi, M.; Samoson, A.; Engelhardt, G.; Grimmer, A. R. *J. Am. Chem. Soc.* **1980**, *102*, 4889−4893.
(38) Barron, P. F.; Frost, R. L. *Am. Mineral.* **1985**, *70*, 758−766.
(39) Demarquay, J.; Fraisard, J. *Chem. Phys. Lett.* **1987**, *136*, 314−318.
(40) Tsiao, C. J.; Carrado, K. A.; Botto, R. E. *Microporous Mesoporous Mater.* **1998**, *21*, 45−51.
(41) Yamanaka, S.; Takahama, K. I.; Kuni, K.; Shiotani, M. *Clay Sci.* **1994**, *9*, 149−158.
(42) Sozzani, P.; Bracco, S.; Comotti, A.; Mauri, M.; Simonutti, R.; Valsesia, P. *Chem. Commun.* **2006**, 1921−1923.
(43) Ferreira, E. S. B.; Hulme, A. N.; McNab, H.; Quye, A. *Chem. Soc. Rev.* **2004**, *33*, 329−336.
(44) Doménech, A.; Doménech-Carbó, M. T.; Sánchez del Río, M.; Vázquez de Agredos Pascual, M. L.; Lima, E. *New J. Chem.* **2009**, *33*, 2371−2379.